Published in final edited form as:
Mol Genet Metab. 2014 May ; 112(1): 30–39. doi:10.1016/j.ymgme.2014.02.014.

Complex changes in the liver mitochondrial proteome of short chain acyl-CoA dehydrogenase deficient mice

Wei Wang[a,b,*], **Al-Walid Mohsen**[c], **Guy Uechi**[d], **Emanuel Schreiber**[d], **Manimalha Balasubramani**[d], **Billy Day**[d], **M. Michael Barmada**[b], and **Jerry Vockley**[b,c,e]

[a]Shanghai Institute of Medical Genetics, Shanghai Children's Hospital Shanghai Jiaotong University, Shanghai, China

[b]Department of Human Genetics, Graduate School of Public Health, University of Pittsburgh, Pittsburgh, USA

[c]Division of Medical Genetics, Children's Hospital of Pittsburgh, Pittsburgh, USA

[d]Genomics and Proteomics Core laboratories, University of Pittsburgh, Pittsburgh, USA

[e]Department of Pediatrics, School of Medicine, University of Pittsburgh, Pittsburgh, USA

Abstract

Short-chain acyl-CoA dehydrogenase (SCAD) deficiency is an autosomal recessive inborn error of metabolism that leads to the impaired mitochondrial fatty acid β-oxidation of short chain fatty acids. It is heterogeneous in clinical presentation including asymptomatic in most patients identified by newborn screening. Multiple mutations have been identified in patients; however, neither clear genotype–phenotype relationships nor a good correlation between genotype and current biochemical markers for diagnosis has been identified. The definition and pathophysiology of this deficiency remain unclear. To better understand this disorder at a global level, quantitative alterations in the mitochondrial proteome in SCAD deficient mice were examined using a combined proteomics approach: two-dimensional gel difference electrophoresis (2DIGE) followed by protein identification with MALDI-TOF/TOF and iTRAQ labeling followed by nano-LC/MALDI-TOF/TOF. We found broad mitochondrial dysfunction in SCAD deficiency. Changes in the levels of multiple energy metabolism related proteins were identified indicating that a more complex mechanism for development of symptoms may exist. Affected pathways converge on disorders with neurologic symptoms, suggesting that even asymptomatic individuals with SCAD deficiency may be at risk to develop more severe disease. Our results also identified a pattern associated with hepatotoxicity implicated in mitochondrial dysfunction, fatty acid metabolism, decrease of depolarization of mitochondria and mitochondrial membranes, and swelling of mitochondria, demonstrating that SCAD deficiency relates more directly to mitochondrial dysfunction and alteration of fatty acid metabolism. We propose several candidate molecules that may serve as markers for recognition of clinical risk associated with this disorder.

*Corresponding author at: Shanghai Institute of Medical Genetics, Shanghai Children's Hospital, Shanghai Jiaotong University, Shanghai, China. Fax: +86 21 62475476. wangwei@shchildren.com.cn (W. Wang).

Appendix A. Supplementary data

Supplementary data to this article can be found online at http://dx.doi.org/10.1016/j.ymgme.2014.02.014.

Keywords

Mitochondrial proteomics; Short chain acyl-CoA dehydrogenase deficiency; Deficient mice; Fatty acid beta-oxidation; Pathways analysis; Network analysis

1. Introduction

Short chain acyl-CoA dehydrogenase (SCAD) is a member of the acyl-CoA dehydrogenase (ACAD) family of enzymes that catalyze the initial reaction of the mitochondrial fatty acid oxidation (FAO) spiral leading to sequential cleavage of two carbon units. FAO serves as an important energy source for the body during times of fasting and metabolic stress. Electrons from reduced SCAD are passed to the electron transfer flavoprotein and then directed into the electron transport chain via electron transfer flavoprotein-ubiquinone oxidoreductase [1]. SCAD is a homotetrameric enzyme encoded in the nuclear genome that functions in mitochondria. It shares structural and functional similarity with other ACADs, each of which has a unique pattern of substrate utilization [2,3]. The human *ACADS* gene is located on chromosome 12q22-qter and spans approximately 13 kb, consisting of 10 exons [4]. The mouse *ACADS* gene maps to chromosome 5 at the Bed-1 locus, and is a compact, single-copy gene approximately 5 kb in size also containing 10 exons [5]. An SCAD deficient Balb/cByJ mouse has been described and is due to a 278-bp deletion at the 3′ end of *ACADS* gene leading to reduced steady-state levels of SCAD mRNA [6].

Short-chain acyl-CoA dehydrogenase deficiency (SCADD) is an inborn error of metabolism that leads to impaired mitochondrial β-oxidation of fatty acids with a carbon backbone length of 4 or 6 carbon units. SCADD results in the accumulation of butyryl-CoA, which in turn leads to the excess production of butyrylcarnitine, butyrylglycine, ethylmalonic acid (EMA), and methylsuccinic acid in blood, urine, and cells [7]. It was originally identified in symptomatic children and adults with heterogeneous symptoms including metabolic acidosis, ketotic hypoglycemia, epilepsy, myopathy, hypotonia, developmental delay and behavioral changes [8,9]. This deficiency was originally thought to affect approximately 1 in 40,000–100,000 newborns, but with the widespread implementation of expanded newborn screening programs through tandem mass spectrometry measurement of acylcarntines in blood spots; additionally, mostly asymptomatic SCAD deficient infants have been identified [10]. The clinical heterogeneity seen in SCADD raises a fundamental question about what (if any) pathophysiologic changes are induced by deficiency of this enzyme. It is clear that biomarkers currently characterized in SCADD patients, including increased urinary EMA and butyrylglycine, increased plasma butyrylcarnitine, and decreased SCAD activity, are not sufficient to predict the development of clinical symptoms and disease severity. Thus, additional biomarkers to categorize effects of SCADD would be of great value.

Approximately 70 genetic variations have been identified in the *ACADS* gene in symptomatic and asymptomatic individuals [10]. No clear genotype–phenotype relationships have been seen in either clinical patients or those identified through newborn screening. Nor is there a good correlation between genotype and the biochemical characteristics of EMA and butyrylglycine excretion [11]. Decreased SCAD activity in skin fibroblasts or muscle is

not a good predictor of clinical symptom. In vitro studies suggest an increase in oxidative stress and protein misfolding in SCADD cells, but in total, the clinical relevance of the biochemical defect and the need to treat affected individuals remain unclear [12–16] Most of the biochemical findings in SCADD mice parallel those seen in the human disease, including organic aciduria with excretion of EMA, methylsuccinic acids and N-butyrylglycine, and development of a fatty liver upon fasting or dietary fat challenge [17]. In contrast to the complicated genetic situation in humans with SCADD mutations, the SCAD deficient mouse provides an excellent model to study pathogenesis of this disease in vivo in a homogenous genetic background.

Proteomics takes a broad, comprehensive and systematic approach to understanding biology, bypassing several inherent limitations to gene expression profiling and genotyping in understanding disease mechanisms. Several approaches have been developed for quantitatively assessing the proteome and comparing differences between the healthy and diseased states. Two-dimensional gel difference electrophoresis (2DIGE) allows comparison of multiple 2D-gels and samples to be analyzed concurrently on the same gel. Compared with conventional two dimensional gel electrophoresis, DIGE shortens the procedure, minimizes the effect of gel to gel variation, and has a large dynamic range allowing differential analysis of abundant proteins, as well as proteins present at low concentration [18]. Isobaric tag for relative and absolute quantification (iTRAQ) has recently come into a more general use in quantitative proteomics [19]. It employs incorporation of 4 to 8 different mass labels into peptides in different samples that can then be compared in one experiment. Labeling multiple peptides per protein increases confidence in identification and quantitation. In this study, we employed both approaches to generate complementary quantitative information on changes in the mitochondrial proteome in SCAD deficient mice compared to wild type animals, and explore novel potential protein markers of disease pathogenesis and severity. Characterization of such changes has the potential to offer new insights into the disease mechanism and provide novel markers for diagnosis.

2. Materials and methods

2.1. Mice

SCAD deficient and wild type BALB/cByJ mice were originally purchased (Jackson Laboratory) at age of 4–5 weeks, and further propagated in the animal facilities at the UPMC Children's Hospital of Pittsburgh. All mice were maintained in a pathogen-free environment, complying with standard housing procedures. Three or five male offspring mice for each genotype were obtained before tissue harvest. All animals were sacrificed at age 6–8 weeks following standard protocols approved by the Institutional Animal Care and Use Committee of the University of Pittsburgh. Tissues were removed immediately after rapid euthanasia with CO_2.

2.2. Isolation of mitochondria

Freshly removed liver was finely minced in ice cold isolation buffer A (225 mM mannitol, 75 mM sucrose, 10 mM HEPES free acid, 10 mM EDTA, pH 7.4), then gently homogenized with a glass Dounce homogenizer in isolation buffer B (225 mM mannitol, 75 mM sucrose,

10 mM HEPES free acid, 0.1% BSA fatty acid free, 10 mM EDTA, pH 7.4) with the addition of 10 μl/ml Halt™ protease inhibitor cocktail (Pierce). The homogenate was centrifuged at 1300 ×g (10 min). A mitochondria pellet was obtained by centrifugation at 10,000 ×g (10 min), and then was resuspended in 12% Percoll solution (Sigma). The mitochondrial band between the 30% and 70% layers was acquired after centrifugation at 62,000 ×g (35 min). Purified mitochondria were collected by centrifugation at 10,000 ×g for 10 min and pellets were stored at −80 °C for use in iTRAQ labeling. The overall experimental workflow is shown in Fig. 1.

2.3. Preparation of mitochondrial protein for DIGE analysis

Mitochondrial protein was extracted immediately after isolation using M-PER Mammalian Protein Extraction Reagent (Pierce). 10 μl/ml of Halt™ protease inhibitor cocktail (Pierce) and 1 μl/ml phosphatase inhibitor cocktail 2 (Sigma) were added to extraction buffer. After removal of cellular debris, protein samples were treated with the 2D Clean-up Kit (GE Health Care) according to manufacturer's instructions. Protein concentration was measured with 2-D Quant Kit (GE Health Care) according to manufacturer's instructions.

2.4. Cy-dye labeling

Stock solutions of PrCy3-N-hydroxysuccinimide ester and MeCy5-N-hydroxysuccinimide ester (Cy3 and Cy5, respectively) were prepared as described [20]. Equal amounts of protein samples from SCAD deficient and wild type mice were individually labeled in a reciprocal manner with equal volumes of Cy3 or Cy5. An equal amount of sample from each genotype mouse was labeled with cyanine dye 2 (Cy2) (GE Health Care) as an internal standard. The labeling reaction was incubated on ice in the dark for 30 min, and was terminated with 1 μl of 40% aqueous methylamine, pH 8.0 [21].

2.5. Difference gel electrophoresis (DIGE)

Each labeled protein sample was dissolved in sample buffer (7 M urea, 2 M thiourea, 2% amidosulfobetaine-14, 10 mg/ml DTT and 1% pharmalytes 3–11). Paired protein samples from deficient and wild type mice were mixed together for subsequent isoelectric focusing on Immobiline DryStrips (24 cm, pH 3–11 nonlinear 3–11 NL) (GE Healthcare). After active rehydration for 10 h at 30 V, IEF was performed on an Ettan IPGphor II system (GE Healthcare) at 300 V for 30 min, 500 V for 30 min, 1000 V for 1h and up to 80,000 Vh, and then maintained at 30 v as needed. Each strip was equilibrated in 50 mM Tris–HCl pH 8.8, 6 M urea, 30% glycerol, 2% sodium dodecyl sulfate (SDS), and 100 mg DTT for 10–15 min. After additional alkylation with 250 mg iodoacetamide, strips were placed on freshly made 12.5% SDS-polyacrylamide gels (SDS-PAGE). Resolved proteins were separated with a vertical Ettan DALTsix electrophoresis system (GE Healthcare) in a running buffer of 1× TGS (Tris–glycine–SDS) (Bio-Rad).

Gels were visualized and evaluated on a Typhoon 9400 Variable Imager (GE Healthcare). Cy3 images were scanned with a 532 nm laser and a 580 nm band pass BP30 emission filter, Cy5 images were scanned with a 633 nm laser and a 670 nm-BP30 emission filter and Cy2 images were scanned using a 488 nm laser and an emission filter of 520 nm BP40. All gels were scanned at 100 μm pixel size for the best resolution. Photomultiplier tube voltage was

set to ensure a maximum pixel intensity between 40 and 60,000 pixels. A focal plane of +3 mm b/c of glass plates was chosen. ImageQuant v5.2 (GE Healthcare) was used to crop the images to exclude the nonessential information prior to image analysis.

Individual images corresponding to Cy2-, Cy3-, and Cy5-labeled samples from each gel were analyzed using DeCyder DIA v5.2 (GE Healthcare). The normalized volume ratio of each spot was compared in each gel between a Cy3- or Cy5-labeled sample to the corresponding Cy2 signal using differential in-gel analysis module. The estimated number of spots for each co-detection procedure was set to 2000. An exclusion filter was used along with manual exclusion of the control spots by inspection. A BVA module incorporated in DeCyder software was used to match multiple images from individual gels and provide statistical data on differential protein expression levels. Student's t-test was selected to compare differences in protein levels between matched spots at a significance of $p \leq 0.05$. A standardized average spot volume ratio exceeding 1.3 fold change in SCAD deficient mice was selected as the minimum to pursue further analysis. Visible spots with Coomassie blue stain were picked and subjected to mass spectrometric analysis.

2.6. Identification of differentially expressed proteins from DIGE analysis

Protein spots that differed on DIGE between deficient and wild type animals were manually retrieved and digested with trypsin. Gel plugs were destained with 100 μl of 50% methanol, 50 mM ammonium bicarbonate and dehydrated with 100 μl of 100% acetonitrile for 20 min. After drying in a vacufuge (eppendorf), samples were digested with 12 μl of a 20 μg/ml trypsin solution (100 μM HCl, 25 mM ammonium bicarbonate, 10% acetonitrile) and incubated at 37 °C overnight with gentle shaking. Supernatants were transferred to 0.5 ml eppendorf tubes and were extracted twice at room temperature with 50 μl of 50% acetonitrile, 1% TFA for 1 h. Extracts were combined and dried in a vacufuge at room temperature. Samples were stored overnight at −20 °C. Dried peptides from in-gel digestion were dissolved in 3 μl of 50% acetonitrile, 0.3% TFA and mixed with 3 μl of freshly prepared matrix solution (10 mg/ml α-cyano-4-hydroxy-cinnamic acid in 50% acetonitrile, 0.3% TFA); 0.6 μl of the mixture was spotted onto a MALDI plate in quadruplicate (Applied Biosystems). Peptides derived from each protein spot were analyzed using a 4700 Proteomics Analyzer (Applied Biosystems). The reflector positive ion mode acquisition and processing methods were chosen to collect peptide spectra in the mass range of 800–4000 Da. Minimum s/n filter was set to 10 and mass exclusion tolerance was set to 50 ppm. The highest ten intensity peptides were selected for analysis using MS/MS acquisition mode of 1 kV positive ion and the processing method with a mass exclusion tolerance of 100 ppm. Data were processed on a GPS Explorer Workstation (Applied Biosystems) and 4000 Series Explorer software v 3.5. MASCOT algorithm v2.2.03 (Matrix Science) was used to search the Mass Spectrometry Protein Sequence DataBase (MSDB). MASCOT parameters were set as follows: searching *Mus* species only, tolerance of one missed trypsin cleavage per peptide, allowance of cysteine modification by acrylamide, oxidation of methionine, carbamidomethyl oxidation peptide charge of +1, precursor tolerance of 100 ppm, and MS/MS fragment tolerance of 0.2 Da. MS/MS peak filtering was set as mass 60 Da to 20 Dabelow precursor mass. Protein identifications (ID scores) were accepted when scores

were above 65 ($P < 0.05$). The identification of a specified protein was considered reliable if at least 3 of 4 quadruplicate spots had an ID score ≥100.

2.7. Preparation of mitochondrial protein for iTRAQ labeling experiments

Mitochondrial pellets isolated were suspended in sample buffer containing 0.5 M triethylammonium bicarbonate buffer (TEAB, pH 8.5), 0.1% SDS at 4 °C. Samples were sonicated 3 times (10 s, 4 °C). Protein concentration was measured using BCA protein assay reagent (Thermo Fisher Scientific, Inc.) according to the manufacturer's instructions.

2.8. iTRAQ labeling

10 μg of protein from each genotype mouse were precipitated with acetone and resuspended in 0.5 M TEAB and 0.5% Rapigest (Waters). Protein samples were denaturated, reduced, alkylated, and digested according to manufacturer's protocol (Applied Biosystems). Four iTRAQ reagents (Applied Biosystems) with mass labels of 114, 115, 116 and 117 Da were used to separately label samples from either deficient or wild type mice. Each sample was labeled twice for each experiment, and a total of 3 experiments were performed with the tagged samples in a reciprocal manner (supplemental Table). Equal amounts of pooled samples from two of the same genotype mice were used as an individual sample. Rapigest detergent was degraded by adding 300 μl of 0.5% formic acid in H_2O (4 °C overnight). Samples were dried by vacuum and reconstituted in 20 μl of 10 mM potassium phosphate (pH 3.0), 25% acetonitrile (ACN). Reporter ions were checked to ensure that the samples were labeled correctly. All of the iTRAQ labeled peptide samples were then mixed for fractionation.

2.9. Strong cation exchange fractionation

PolySULFOETHYL Macro-Spin columns (12 μm, 300 Å, 50–450 μl (The Nest Group Inc.) were pretreated with methanol and water, and then equilibrated with 10 mM potassium phosphate, pH 3.0 and 25% ACN. Samples were diluted in 10 mM potassium phosphate, 25% ACN, pH 3.0, and then loaded onto the column. Six fractions were collected by stepwise elution with 20 mM KCL, 40 mM KCL, 80 mM KCL, 100 mM KCL, 200 mM KCL and 400 mM KCL in 10 mM potassium phosphate, 25% ACN, pH 3.0. Eluted fractions were lyophilized, resuspended in 0.5% trifluoroacetic acid, 5% ACN, and desalted using a PepClean C-18 column (Pierce) according to manufacturer's instructions.

2.10. Nano-LC separation

Peptides were further separated using an RP LC-Packing Ultimate system (Dionex) with a trap column (300 μm i.d. × 5 mm, PepMap100 C18 material 5 μm, 100 Å) and an analytical column (75 μm i.d. × 100 mm, PepMap100 C18 material 3 μm, 100 Å) (Dionex). An LC gradient of 0–56% buffer B in 115 min, 56%–100% B in 5 min, and 100% B for 5 min, followed by re-equilibration to starting conditions, all at a flow rate of 300 nl/min, was employed. Buffer A was 5% ACN, 0.1% TFA, and buffer B was 85% ACN, 5% isopropyl alcohol and 0.1% TFA. A BSA digest standard (Michrom Bioresources) was run on the LC system as a control prior to and following sample runs. BSA peptides were eluted using a gradient of 0–56% B in 30 min, 56%–100% B in 5 min, and 100% B for 5 min, all at a flow

rate of 300 nl/min. Eluted fractions were collected using a Probot™Micro Fraction Collector system (Dionex) and spotted on an ABI 4800 LC-MALDI metal target plate at 30 second intervals with a 16 × 48 array. A total of 576 spots were collected for each strong cation exchange (SCX) fraction samples and 192 spots were collected for each fraction of control BSA peptides. During the LC run, 10 mg/ml α-cyano-4-hydroxy cynnamic acid (CHCA) with 10 mM ammonium citrate dibasic and 10 fM angiotensin II in 85% ACN, 0.1% TFA were mixed with the flow and co-spotted on the plate using a μTee mixer at a flow rate of 1.5 μl/min.

2.11. Mass spectrometry of iTRAQ labeled peptides

A 4800 analyzer equipped with TOF/TOF ion optics (ABSciex) was used to analyze MALDI target plates and MS–MS/MS data were acquired using 4000 Series Explorer software, version 3.5.1. The instrument was calibrated before each run. The operating mode of MS was set to MS reflector positive. MS spectra were acquired from 900 to 4000 Da with a focus mass of 2000 Da to determine the mass of precursor ions of interest with precursor tolerance of 0.25 Da. MS spectra were internally calibrated using angiotensin II that was spiked into matrix. The top 10 high intensity peptide precursors above a S/N filter of 20 were selected for fragmentation by collision induced dissociation at 2 kV in positive mode with an accumulation of 2000 shots for each spectrum.

2.12. Protein quantification and identification of iTRAQ labeled samples

Database searches were performed with ProteinPilot™ Software 2.0 (ABSciex) using a combined search with all 6 fractions. Searches were performed using the International Protein Index (IPI) database v3.68 (mouse). Parameters were set to “ID search” and were focused on biological modifications, iTRAQ labeling of N-terminus and lysine residues, cysteine modification by methylmethanethiosulfonate (MMTS) and digestion by trypsin, and included bias and background correction. Isoform specific identification and quantification were done by excluding all shared peptides and including only unique peptides. Proteins were determined at 5% FDR and more stringent criteria of reporting proteins by correcting bias and background were applied. Furthermore, protein identifications were considered to be correct based on the following selection criteria: a protein had at least 2 peptides with an ion score above 99% confidence; only unique peptides with corresponding peaks of iTRAQ labels were included in the quantitative analysis; error factor was lower than 1 (Supplementary files). Proteins with protein score (ProtScore) >1.3 (unused, $p < 0.05$; 95% confidence) were included in further statistical analysis.

2.13. Biostatistical analysis on iTRAQ labeled samples

Outliers (>1.3 fold changed SCAD protein expression in the same experiment) were excluded by plotting the data distribution before normalization. All obtained values of iTRAQ labeled proteins in each of three independent experiments were summed and then averaged as the reference baseline value in that experiment. The quantification value of each protein was then normalized by obtaining the ratio of the iTRAQ quantification value to the reference value. The reference value was set to 1. Fold changes of protein expression in mutants were recalculated and averaged from three experiments. Student's t-test ($p < 0.05$)

was used to test the difference between mutant and wild type for each protein. Proteins with expression altered >1.3 fold or <0.7 fold in at least 2 independent experiments were set as the cutoff of changed values.

2.14. Pathway and network analysis

All differentially expressed proteins from two proteomic analysis approaches with their gene symbol names as identifiers were subjected to Ingenuity Pathways Analysis software (Ingenuity Systems, www.ingenuity.com). Filters and general settings were set to consider all molecules as well as both direct and indirect relationships. The *taxae* of human and mouse and all data sources were selected. Networks and canonical pathways of focus genes and associations to biological functions (and/or diseases) were then algorithmically generated. Toxicity analysis function incorporated in IPA software was utilized to assess the secondary physiologic impact of primary *ACADS* gene deficiency. In this analysis, we essentially defined SCAD deficiency as a “toxin”, assessed secondary changes identified in mitochondrial proteome, and assigned them to functional pathways as with more traditional small molecule studies. Biomarker analysis function was originally incorporated in IPA software to identify disease or predict the development of symptoms. We utilized this function to identify and prioritize promising molecular biomarker candidates from differentially expressed proteins in SCAD deficient mice. A biomarker filter was selected to focus on contextual information related to human and mouse genes associated with known diseases.

2.15. Western blotting

Equal amounts of 50 μg or 100 μg of mitochondrial protein from wild type and deficient mice were separated by 10% Bis–Tris SDS polyacrylamide gels in MOPS buffer (Bio-Rad, Hercules, CA). Separated proteins were transferred to 0.2 μm nitrocellulose membrane (Bio-Rad) using a TE Series Transphore Electrophoresis Unit (Hoefer Scientific Instruments, Holliston, MA). The membrane was immunoblotted with desired antibodies. Primary antibodies used were SCAD [22,23], Complex III subunit core 2 (Mitoscience, Eugene, OR), SCP2, and HSP60 (Santa Cruz Biotech, Santa Cruz, CA). In each gel, SDH (Complex II) antibody (Santa Cruz Biotech) was used as a loading control. The secondary antibody conjugated to horseradish peroxidase included rabbit anti-goat IgG or anti-mouse IgG (Santa Cruz Biotech) was chosen according to the primary antibody used. Bound secondary antibody was detected with western blotting Luminol Reagent (Santa Cruz Biotech) and scanned using Fujifilm LAS-3000 (Fujifilm Medical Systems, Stamford, CT). Band intensity was quantitated from a scanned blot image using ImageJ software v1.46 (imagej.nih.gov).

3. Results

To characterize mitochondrial proteome changes related to SCADD, DIGE analysis of isolated mitochondria followed by protein identification with matrix assisted laser desorption ionization time of flight/time of flight (MALDI-TOF/TOF) mass spectrometry was first utilized. iTRAQ labeling followed by peptide separation and identification with liquid chromatography (LC)-MALDI-TOF/TOF was then performed. An overview of the

experimental approach is shown in Fig. 1. A total of 49 proteins with differential expression in SCAD deficient mice were identified, including a variety of energy metabolism related proteins.

3.1. Differentially expressed proteins in SCAD deficient mice identified with DIGE analysis

Biological Variation Analysis (BVA) incorporated in DeCyder detected 161 matched spots among all gels. Statistically significant ($p \leq 0.05$) increases in 12 (7.5%) spots and decreases in 16 spots (9.9%) (student's t-test, $p \leq 0.05$) were identified in mitochondria from SCAD deficient mice compared to wild type mice. Spots with >1.3 fold change are depicted on a representative 2DIGE gel image (Fig. 2). A Mascot database search of MS spectra resulted in the identification of 10 proteins obtained from quadruplicate MALDI spots in individual gels. All proteins identified were located in mitochondria. Sterol carrier protein 2 and sterol carrier protein X identified in two different positions (spot 1 and spot 2) are the same protein with synonymous names in the UniProt database (non-specific lipid-transfer protein). Spot 9 was identified as beta-alanine oxoglutarate amino-transferase, synonymously named 4-aminobutyrate aminotransferase. Catalase/mutant catalase assigned to 3 spots (spots 5, 6, and 14) has long been thought to be a typical peroxisomal protein, however, recent findings have shown that it is actually more abundant in rat liver mitochondria than in peroxisomes [24]. Here, our results also suggest it is abundant in mouse liver mitochondria.

3.2. Differentially expressed proteins in SCAD deficient mice identified with iTRAQ labeling

Among proteins differentially expressed in SCAD deficient mice, 38 proteins were classified as being increased by 1.3-fold or decreased by 0.7-fold in at least 2 experiments (supplemental Table 3). Some proteins are not recognized as being localized to the mitochondria, whereas others are reported to localize to multiple organelles. Analysis of biological functions associated with up-regulated proteins revealed that 5/19 (26%) of them are involved in amino acid metabolism. 2/19 (10%) proteins are related to fatty acid oxidation, and 2/19 (10%) proteins are involved in the tricarboxylic acid (TCA) cycle. Down-regulated proteins included 7 proteins belonging to complexes I, III and IV of the mitochondrial electron transport chain. Only one down-regulated protein was associated with fatty acid oxidation. 7/38 altered proteins were not associated with clear or defined functions.

3.3. Summation of differentially expressed proteins in SCAD deficient mice

48 differentially expressed proteins identified by iTRAQ labeling experiments were further grouped according to their basic biological function annotation in UniProt/Swiss-Prot (supplemental Table 3). Among the 25 up-regulated proteins, 4 (16%) were associated with fatty acid metabolism and 9 (36%) were associated with amino acid metabolism (Fig. 3). Among the 21 down-regulated proteins, one protein was associated with fatty acid metabolism and one protein was associated with amino acid metabolism. Most of the identified down-regulated proteins (29%) were involved in oxidative phosphorylation (OXPHOS) including components of complexes I, III, and IV of the electron transport chain (ETC.). While complex V was observed to be up-regulated with DIGE analysis, it was identified as being slightly down-regulated, though not low enough to meet the minimum cutoff selection criterion, with iTRAQ. Two enzymes/proteins involved in TCA cycle were

up-regulated but none of the enzymes associated with the TCA cycle were down-regulated. Though, none of the identified proteins was consistently seen in both approaches, several proteins were identified as being altered in DIGE analysis and one of the iTRAQ labeling experiments, but didn't meet our defined criteria in the iTRAQ experiment. These are listed in supplemental Table 4.

3.4. Western blot analysis

Three proteins of interest relative to mitochondrial metabolism were selected to validate our findings (Fig. 4). Cytochrome b–c1 complex subunit 2 (UQCR2) was slightly decreased in iTRAQ experiments and on western blots. Sterol carrier protein 2 (SCP2) was significantly increased in SCAD deficient mice in DIGE analysis but only slightly increased on western blots. HSP60 (heat shock protein 60) was slightly increased (1.2 fold) on western blots. In proteomic experiments, one isoform of HSP60 was identified as being altered. The level of the housekeeping protein succinate dehydrogenase was constant as measured either by western blot or proteomic analysis. Not surprisingly, SCAD was almost absent in western blot analysis, though it was only decreased by 3–4 fold on DIGE gels. (See Fig. 4.)

3.5. Pathway and gene ontology analysis

Ingenuity Pathway Analysis (IPA) was used to classify proteins altered in SCAD deficient mice into different functional groups and to predict altered cellular activities and related pathways. Among the 37 of the 48 altered proteins used for canonical pathway analysis, 20 proteins/enzymes were linked by specific networks. The most significant network was “lipid metabolism, molecular transport and small molecules biochemistry” (Fig. 5) composed of 16 proteins identified experimentally and 19 proteins inferred from the IPA database. All of the 5 down-regulated and 8 up-regulated proteins were enzymes. This network is linked through literature reports by several transcription regulators and transporters, though they were not identified in our experiments. Only two mitochondrial transporters were detected experimentally, both of which were up-regulated.

IPA also highlighted several canonical pathways as being affected in SCAD deficient mice. The most affected pathway was that of “branched chain amino acid metabolism” (Fig. 6). Nine proteins were involved in “mitochondrial dysfunction”, comprising 7.7% of all molecules in this pathway ($p < 0.001$). Seven proteins in the “mitochondrial dysfunction” pathway were down-regulated in SCAD deficient mice, 6 of which were involved in OXPHOS. In addition to SCAD, only one protein (encoded by ABAT) was decreased, while the other 6 proteins were increased (1.62–2.60 fold). Another top-related canonical pathway was fatty acid metabolism, which also includes proteins in the “OXPHOS” pathway. Most of the proteins associated with the fatty acid pathway were increased in SCAD deficient mice. Proteins in pyruvate metabolism were consistently up-regulated, while fatty acid metabolism, mitochondrial dysfunction and OXPHOS were altered in a complex pattern (not simply either up-or down-regulated).

Altered proteins were also analyzed relative to association with IPA related disease groups (Table 1). Not surprisingly, the largest number of altered proteins (18/37), including 8 down-regulated proteins and 9 up-regulated ones, were associated with metabolic diseases.

Among them, 4-aminobutyrate transaminase was significantly decreased. It is interesting and encouraging that 6 proteins (NDUFS7, GLUD1, MDH2, OTC, ABAT and HSPD1) were associated with neurologic disease. (See Table 1.)

The toxicity analysis function in IPA was utilized to identify potentially relevant secondary changes related to SCADD and provide additional insight into pathologic alterations induced by the deficiency (Table 1). Of note, a pattern associated with hepatoxicity was seen as indicated by alterations of 5 proteins in “mitochondrial dysfunction”, “fatty acid metabolism”, “decrease of depolarization of mitochondria and mitochondrial membrane and swelling of mitochondria” groups (Fig. 7). This analytical tool does not provide parameters to assess specific impact on skeletal muscle, thus, potential toxicity in this organ was not identifiable.

Finally, biomarker analysis using IPA identified and prioritized several potential molecular biomarker candidates among the differentially expressed proteins. To magnify the significance of the results, the analysis was filtered for all body fluids where a biomarker has previously been used in the diagnosis of, or was associated with efficacy, prognosis, progression, response or safety of a specific disease. We first identified 7 candidate markers that have been associated with related diseases (Table 2). Five of them were up regulated. Two decreased enzymes encoding CPT2 and GLUD1 were identified. However, when applying more restricted filter parameters on human or mouse and including only tissue specificity of liver, no biomarker candidates were identified.

4. Discussion

The clinical relevance of and need for therapy in SCADD remains controversial. A wide array of symptoms has been reported in patients, but the majority of infants identified through newborn screening [11, 25–27]. The definition of this condition and its physiologic ramifications remain unclear. It is possible that SCADD represents a risk factor for the development of neurologic disease, has an unrecognized later onset phenotype, creates secondary changes that can be problematic, or is just a biochemical phenotype rather than a disease. The purposes of this study were to gain further insight into systemic changes induced by SCAD deficiency and to identify biomarkers to predict the development and severity of symptoms by surveying changes in the mitochondrial proteome of SCAD deficient mice.

We first profiled proteomic changes in liver mitochondria from SCAD deficient mice. Our experiments revealed a broad pattern of mitochondrial dysfunction beyond fatty acid oxidation induced by SCAD deficiency. A considerable number of proteins related to energy metabolism in fatty acid metabolism, amino acid metabolism and TCA cycle were dysregulated in SCADD mice. These include carbamylphosphate synthase I (CPS1), carnitine palmitoyltransferase 2 (CPT2), pyruvate carboxylase (PC) and hypolipidemia (sterol carrier protein 2; SCP2). These changes may, in part, explain heterogeneous symptoms in SCAD deficiency. These changes also imply that short chain fatty acids are less available to produce energy, with resultant compensation through generation of energy from other sources. While these compensatory changes may overcome the primary

deleterious effects of impaired energy production in SCAD deficiency, it provides opportunities for variable expression of other genes to impact phenotype. The physiologic cause of these changes and their effect on cellular metabolism are unknown. They underscore the complexity of secondary alterations that must be taken into account to fully understand the physiologic effects of a single gene defect such as SCADD, providing further impetus to better characterize these changes and their roles in the development of symptoms in humans.

Multiple energy metabolism related pathways were altered, indicating that a more complex mechanism for development of symptoms may exist. The diversity of other pathways altered in SCAD deficient mice suggests that differential compensatory or secondary deleterious effects may play a predominant role in determining the pathophysiology of SCADD. A decrease of almost all complexes in electron transport chain implies that less efficient fatty acid oxidation may be magnified by a secondary defect in OXPHOS, and thus ATP production. In addition to one subunit of NADH dehydrogenase (iron–sulfur protein 7), we demonstrated the reduction of 5 subunits of other respiratory chain complexes and complex III binding protein (cytochrome b–c1 complex subunit 7) encoded by *UGRCB*. It has been reported that mutations in *UGRCB* gene are associated with mitochondrial complex III deficiency. Mutations in *ACAD9*, another member of the *ACAD* gene family, can lead to either a fatty acid oxidation defect or the deficiency of respiratory chain complex I [28,29]. This correlation between fatty acid oxidation and oxidative phosphorylation is consistent with the recognition that many patients with respiratory chain complex deficiencies accumulate metabolites suggestive of fatty acid-oxidation dysfunction, and the recent description of a multi-functional enzyme complex encompassing all activities of fatty acid oxidation and respiratory chain [23]. However, as many proteins in the mitochondria were approached simultaneously, results obtained may not exactly represent the assembly and status of complex and supercomplexes in OXPHOS. We propose further more extensive study to examine the respiratory chain supercomplexes and their association with the fatty acid oxidation proteins.

Network analysis and pathways reveal that transcription regulators link the energy metabolism pathways are altered in SCADD mice, however most such factors are located in the nucleus or translocate from the cytosol to the nucleus upon mitochondrial stress, and are therefore not expected to be identified in a mitochondrial proteome. For example, SCAD is connected to CPS1 through PPARA and LEP, neither of which is mitochondrial in location. Thus, to understand SCAD deficiency, it becomes necessary to consider functions linked through these regulatory factors in addition to energy pathways.

Most symptomatic SCADD patients reported in the literature have presented with predominantly neurologic manifestations, which are rarely seen in other ACAD defects. Deficiency of the respiratory chain, including abnormalities in NDUFS7, is a common cause of the neurometabolic condition Leigh syndrome [23]. Our disease association analysis identified additional genes involved in neurological disease as being altered in SCAD deficient mice, including GLUD1, MDH2, OTC and ABAT. Deficiencies of these enzymes have been documented in patients with Reye-like symptoms that overlap many disorders of energy metabolism [30,31]. The alteration of 4-aminobutyrate aminotransferase encoded by

ABAT catalyzes the conversion of the inhibitory neurotransmitter GABA to succinic semialdehyde and glutamate. The phenotype of GABA-transferase deficiency includes psychomotor retardation, hypotonia, hyperreflexia, lethargy, refractory seizures and EEG abnormalities [31,32] The pattern of alterations of these enzymes in SCAD deficiency, may in part, at least help explain neurological manifestations in severe SCAD deficient patients. Further assessment of proteins altered in the neurologic disease category in SCADD patients could provide further insight into the role of these changes in the development of clinical symptoms.

Historically, a combination of histopathology and clinical chemistry has been used to estimate the toxicity of a specific treatment, and differentiating toxic effects of treatment from disease-associated changes was problematic. To better characterize the potential clinical relevance of changes in the mitochondrial proteome related to SCAD gene deficiency, the toxicity analysis function of IPA software was utilized. In this analysis, we treated the presence of changed molecules as a pharmacologic agent, and queried the analytical software for evidence of “treatment” toxicity. Here, a pattern of hepatoxicity emerged related to changes in gene/proteins in the functional groups of mitochondrial dysfunction, fatty acid metabolism, decrease of depolarization of mitochondria and mitochondrial membrane, and swelling of mitochondria. Such a toxicity analysis approach should be of general use in studying the pathophysiologic effects of other single gene mutations in genetic models of disease.

Proteomic patterns of secondary damage with the potential to cause pathophysiologic changes seen in this study in SCAD deficient mice are consistent with previous reports. EMA has been shown to cause an increase in oxidative stress in rat cerebral cortex [33]. Overexpression of a variant SCAD protein in astrocytes has been shown to induce mitochondrial changes that were partially reversed by administration of a mitochondrial antioxidant [14]. Similarly, stress response genes were up-regulated in a cell culture system overexpressing a variant SCAD gene [14].

The novelty of this study lies in the application of proteomic approaches to identify alterations in molecular pathways induced by SCAD deficiency, and provides additional insight into the fundamental pathophysiology of this condition. Multiple experimental details provide robustness to our conclusions. Replicate experiments and complementary proteomic approaches serve to provide confidence in the changes seen, as does verification by western blotting. However, the variability among different experiments, reproducibility issues in the fractionation method utilized, and the proper threshold of expression selected to consider a change to be over- or under expressed must all be carefully considered in interpreting results. Thus, our study focused on only further exploring or describing those proteins detected in replicate experiments. With respect to methodology, we used multiple separation and sample preparation steps in two different methods to identify changed proteins among a complex proteome. The proteins identified as showing differential expression were complementary with only a few overlapping proteins. Of the two methods used, iTRAQ labeling proved to be more sensitive and more robust at generating data for statistical comparisons. Note that mitochondria in this study were isolated by differential centrifugation, a technique that also yields peroxisomes. Moreover, a single protein may

reside in more than one subcellular compartment of the cell. We reported only proteins with high coverage and consistent differences in mitochondrial expression. However, the contribution of these proteins to the overall signal detected by the mass spectrometer was low, indicating that variation of these signals would not affect that of the highest fraction of proteins belonging to the category of mitochondria. The inconsistencies seen between results obtained with DIGE and iTRAQ might derive from the presence of multiple proteins in DIGE spots, as well as differences in sensitivity, signal detection ability and protein integration before detection. Overall, DIGE was less sensitive than iTRAQ but correlated better with western blot analysis; not surprising as both DIGE and western blot share similarities in technique.

Liver is a mitotic tissue with a high rate of cell division and thus, typically, rapid protein turnover and a high level of innate variation in protein abundance. The range of biological variation that can be tolerated by the cell depends on the individual protein. Such inherent biological variation cannot be eliminated completely, but its effect on experimental outcome can be minimized by analyzing multiple samples in each genotypic group and pooling of samples. Our proteomic analysis evaluated both proteins encoded in the nuclear genome and imported into mitochondria as well as those encoded on the mitochondrial chromosome. Thus, the changes identified in mutant mice reflect a compilation of all dynamic changes including gene expression as well as protein modification and the processes of mitochondrial targeting, import, and protein folding. It is important to note that a protein must be relatively abundant to be detected by the techniques used in this study, although additional changes can be underrated by network analysis.

One goal of the current study was to identify biomarkers to distinguish asymptomatic SCAD deficiency from individuals at risk to develop symptoms and thus serve as markers for adjunct diagnosis and monitoring of therapy. Relevant biomarkers associated with other related diseases were then prioritized from all differentially expressed proteins. Among the proteins thus identified from those altered in SCADD mice, acetyl-CoA acyltransferase 2 (ACAA2), carnitine palmitoyltransferase 2 (CPT2), and glutamate dehydrogenase (GLUD1) are of interest. Future studies are necessary to determine if either one or combination of these markers would better than the current biochemical markers (urinary EMA and butyrylglycine and plasma butyrylcarnitine) at predicting severity of disease.

5. Conclusion

We have identified and quantitated changes in the mitochondrial proteome in animals with SCAD deficiency that implicate a complicated process of cellular toxicity with multiply altered pathways and disease associated networks. Additionally, these pathways converge on disorders with neurologic symptoms, suggesting that even asymptomatic individuals with SCAD deficiency may be at risk of developing more severe disease. We propose a complex mechanism in the development of SCAD deficiency resulting in heterogeneous symptoms, and identify candidate biomarkers to explore further as potential indicators of disease severity.

Supplementary Material

Refer to Web version on PubMed Central for supplementary material.

Acknowledgments

These studies were supported in part by NIH grant R01DK54936 (JV) and a fellowship award from the Children's Hospital of Pittsburgh of UPMC Rangos Research Committee (WW). We thank Dr. Steven Ringquist and Ying Lu in Division of Immunogenetics, Children's Hospital of Pittsburgh for technical support in DIGE analysis.

Abbreviations

EMA	ethylmalonic acid
ETC	electron transport chain
FAO	fatty acid oxidation
iTRAQ	isobaric tags for relative and absolute quantification
LC	liquid chromatography
MALDI-TOF/TOF	matrix assisted laser desorption ionization time of flight/time of flight
MS	mass spectrometry
OTC	ornithine transcarbamylase
OXPHOS	oxidative phosphorylation
SCAD	short-chain acyl-CoA dehydrogenase
SCADD	short-chain acyl-CoA dehydrogenase deficiency
SDS-PAGE	sodium dodecyl sulfate-polyacrylamide gels
TCA	tricarboxylic acid
2DIGE	two-dimensional gel difference electrophoresis

References

1. Ghisla S, Thorpe C, Massey V. Mechanistic studies with general acyl-CoA dehydrogenase and butyryl-CoA dehydrogenase: evidence for the transfer of the b-hydrogen to the flavin N(5)-position as a hydride. Biochemistry. 1984; 23:3154–3161. [PubMed: 6466635]
2. Matsubara Y, Indo Y, Naito E, Ozasa H, Glassberg R, Vockley J, Ikeda Y, Kraus J, Tanaka K. Molecular cloning nucleotide sequence of cDNAs encoding the precursors of rat long chain acyl-CoA, short chain acyl-CoA and isovaleryl CoA dehydrogenases: sequence homology of four enzymes of the acyl-CoA dehydrogenase family. J. Biol. Chem. 1989; 264:16321–16331. [PubMed: 2777793]
3. Kim JJ, Miura R. Acyl-CoA dehydrogenases and acyl-CoA oxidases. Structural basis for mechanistic similarities and differences. Eur. J. Biochem. 2004; 271:483–493. [PubMed: 14728675]
4. Corydon MJ, Andresen BS, Bross P, Kjeldsen M, Andreasen PH, Eiberg H, Kolvraa S, Gregersen N. Structural organization of the human short-chain acyl-CoA dehydrogenase gene. Mamm. Genome. 1997; 8:922–926. [PubMed: 9383286]
5. Kelly CL, Wood PA. Cloning and characterization of the mouse short-chain acyl-CoA dehydrogenase gene. Mamm. Genome. 1996; 7:262–264. [PubMed: 8661694]

6. Hinsdale ME, Kelly CL, Wood PA. Null allele at Bcd-1 locus in BALB/cByJ mice is due to a deletion in the short-chain acyl-CoA dehydrogenase gene and results in missplicing of mRNA. Genomics. 1993; 16:605–611. [PubMed: 8325633]
7. Corydon MJ, Gregersen N, Lehnert W, Ribes A, Rinaldo P, Kmoch S, Christensen E, Kristensen TJ, Andresen BS, Bross P, Winter V, Martinez G, Neve S, Jensen TG, Bolund L, Kolvraa S. Ethylmalonic aciduria is associated with an amino acid variant of short chain acyl-coenzyme a dehydrogenase. Pediatr. Res. 1996; 39:1059–1066. [PubMed: 8725270]
8. Amendt B, Green C, Sweetman L, Cloherty H, Shih V, Moon A, Teel L, Rhead W. Short chain acyl-CoA dehydrogenase deficiency: clinical and biochemical studies in two patients. J. Clin. Invest. 1987; 79:1303–1309. [PubMed: 3571488]
9. Kurian MA, Hartley L, Zolkipli Z, Little MA, Costigan D, Naughten ER, Olpin S, Muntoni F, King MD. Short-chain acyl-CoA dehydrogenase deficiency associated with early onset severe axonal neuropathy. Neuropediatrics. 2004; 35:312–316. [PubMed: 15534767]
10. Pedersen CB, Kolvraa S, Kolvraa A, Stenbroen V, Kjeldsen M, Ensenauer R, Tein I, Matern D, Rinaldo P, Vianey-Saban C, Ribes A, Lehnert W, Christensen E, Corydon TJ, Andresen BS, Vang S, Bolund L, Vockley J, Bross P, Gregersen N. The ACADS gene variation spectrum in 114 patients with short-chain acyl-CoA dehydrogenase (SCAD) deficiency is dominated by missense variations leading to protein misfolding at the cellular level. Hum. Genet. 2008; 124:43–56. [PubMed: 18523805]
11. van Maldegem BT, Duran M, Wanders RJA, Niezen-Koning KE, Hogeveen M, Ijlst L, Waterham HR, Wijburg FA. Clinical, biochemical, and genetic heterogeneity in short-chain acyl-coenzyme A dehydrogenase deficiency. JAMA. 2006; 296:943–952. [PubMed: 16926354]
12. Gregersen N, Olsen RK. Disease mechanisms and protein structures in fatty acid oxidation defects. J. Inherit. Metab. Dis. 2010; 33:547–553. [PubMed: 20151199]
13. Pedersen CB, Zolkipli Z, Vang S, Palmfeldt J, Kjeldsen M, Stenbroen V, Schmidt SP, Wanders RJ, Ruiter JP, Wibrand F, Tein I, Gregersen N. Antioxidant dysfunction: potential risk for neurotoxicity in ethylmalonic aciduria. J. Inherit. Metab. Dis. 2010; 33:211–222. [PubMed: 20443061]
14. Schmidt SP, Corydon TJ, Pedersen CB, Bross P, Gregersen N. Misfolding of short-chain acyl-CoA dehydrogenase leads to mitochondrial fission and oxidative stress. Mol. Genet. Metab. 2010; 100:155–162. [PubMed: 20371198]
15. Schmidt SP, Corydon TJ, Pedersen CB, Vang S, Palmfeldt J, Stenbroen V, Wanders RJ, Ruiter JP, Gregersen N. Toxic response caused by a misfolding variant of the mitochondrial protein short-chain acyl-CoA dehydrogenase. J. Inherit. Metab. Dis. 2011; 34:465–475. [PubMed: 21170680]
16. Zolkipli Z, Pedersen CB, Lamhonwah AM, Gregersen N, Tein I. Vulnerability to oxidative stress in vitro in pathophysiology of mitochondrial short-chain acyl-CoA dehydrogenase deficiency: response to antioxidants. PLoS ONE. 2011; 6:e17534. [PubMed: 21483766]
17. Wood PA, Amendt BA, Rhead WJ, Millington DS, Inoue F, Armstrong D. Short-chain acyl-coenzyme A dehydrogenase deficiency in mice. Pediatr. Res. 1989; 25:38–43. [PubMed: 2919115]
18. Ong SE, Foster LJ, Mann M. Mass spectrometric-based approaches in quantitative proteomics. Methods. 2003; 29:124–130. [PubMed: 12606218]
19. Ross PL, Huang YN, Marchese JN, Williamson B, Parker K, Hattan S, Khainovski N, Pillai S, Dey S, Daniels S, Purkayastha S, Juhasz P, Martin S, Bartlet-Jones M, He F, Jacobson A, Pappin DJ. Multiplexed protein quantitation in Saccharomyces cerevisiae using amine-reactive isobaric tagging reagents. Mol. Cell. Proteomics. 2004; 3:1154–1169. [PubMed: 15385600]
20. Unlu M, Morgan ME, Minden JS. Difference gel electrophoresis: a single gel method for detecting changes in protein extracts. Electrophoresis. 1997; 18:2071–2077. [PubMed: 9420172]
21. Beckner ME, Chen X, An J, Day BW, Pollack IF. Proteomic characterization of harvested pseudopodia with differential gel electrophoresis and specific antibodies. Lab. Invest. 2005; 85:316–327. [PubMed: 15654357]
22. Schuck PF, Ferreira Gda C, Tonin AM, Viegas CM, Busanello EN, Moura AP, Zanatta A, Klamt F, Wajner M. Evidence that the major metabolites accumulating in medium-chain acyl-CoA dehydrogenase deficiency disturb mitochondrial energy homeostasis in rat brain. Brain Res. 2009; 1296:117–126. [PubMed: 19703432]

23. Wang Y, Mohsen AW, Mihalik SJ, Goetzman ES, Vockley J. Evidence for physical association of mitochondrial fatty acid oxidation and oxidative phosphorylation complexes. J. Biol. Chem. 2010; 285:29834–29841. [PubMed: 20663895]
24. Jiang XS, Dai J, Sheng QH, Zhang L, Xia QC, Wu JR, Zeng R. A comparative proteomic strategy for subcellular proteome research: ICAT approach coupled with bio-informatics prediction to ascertain rat liver mitochondrial proteins and indication of mitochondrial localization for catalase. Mol. Cell. Proteomics. 2005; 4:12–34. [PubMed: 15507458]
25. van Maldegem BT, Duran M, Wanders RJ, Niezen-Koning KE, Hogeveen M, Ijlst L, Waterham HR, Wijburg FA. Clinical, biochemical, and genetic heterogeneity in short-chain acyl-coenzyme A dehydrogenase deficiency. JAMA. 2006; 296:943–952. [PubMed: 16926354]
26. Gallant NM, Leydiker K, Tang H, Feuchtbaum L, Lorey F, Puckett R, Deignan JL, Neidich J, Dorrani N, Chang E, Barshop BA, Cederbaum SD, Abdenur JE, Wang RY. Biochemical, molecular, and clinical characteristics of children with short chain acyl-CoA dehydrogenase deficiency detected by newborn screening in California. Mol. Genet. Metab. 2012; 106:55–61. [PubMed: 22424739]
27. Wolfe, L.; Jethva, R.; Oglesbee, D.; Vockley, J. Short-chain acyl-CoA dehydrogenase deficiency, in. In: Pagon, RA.; Adam, MP.; Bird, TD.; Dolan, CR.; Fong, CT.; Stephens, K., editors. Seattle WA: GeneReviews, GeneReviews; 2011.
28. Haack TB, Danhauser K, Haberberger B, Hoser J, Strecker V, Boehm D, Uziel G, Lamantea E, Invernizzi F, Poulton J, Rolinski B, Iuso A, Biskup S, Schmidt T, Mewes HW, Wittig I, Meitinger T, Zeviani M, Prokisch H. Exome sequencing identifies ACAD9 mutations as a cause of complex I deficiency. Nat. Genet. 2010; 42:1131–1134. [PubMed: 21057504]
29. He M, Rutledge SL, Kelly DR, Palmer CA, Murdoch G, Majumder N, Nicholls RD, Pei Z, Watkins PA, Vockley J. A new genetic disorder in mitochondrial fatty acid beta-oxidation: ACAD9 deficiency. Am. J. Hum. Genet. 2007; 81:87–103. [PubMed: 17564966]
30. Mitchell RA, Ram ML, Arcinue EL, Chang CH. Comparison of cytosolic and mitochondrial hepatic enzyme alterations in Reye's syndrome. Pediatr. Res. 1980; 14:1216–1221. [PubMed: 7454435]
31. Deshmukh DR, Remington PL. Ornithine carbamyl transferase in Reye's syndrome. Biochem. Med. 1984; 32:337–340. [PubMed: 6517878]
32. Medina-Kauwe LK, Tobin AJ, De Meirleir L, Jaeken J, Jakobs C, Nyhan WL, Gibson KM. 4-Aminobutyrate aminotransferase (GABA-transaminase) deficiency. J. Inherit. Metab. Dis. 1999; 22:414–427. [PubMed: 10407778]
33. Schuck PF, Busanello EN, Moura AP, Tonin AM, Grings M, Ritter L, Vargas CR, da Costa Ferreira G, Wajner M. Promotion of lipid and protein oxidative damage in rat brain by ethylmalonic acid. Neurochem. Res. 2010; 35:298–305. [PubMed: 19757035]

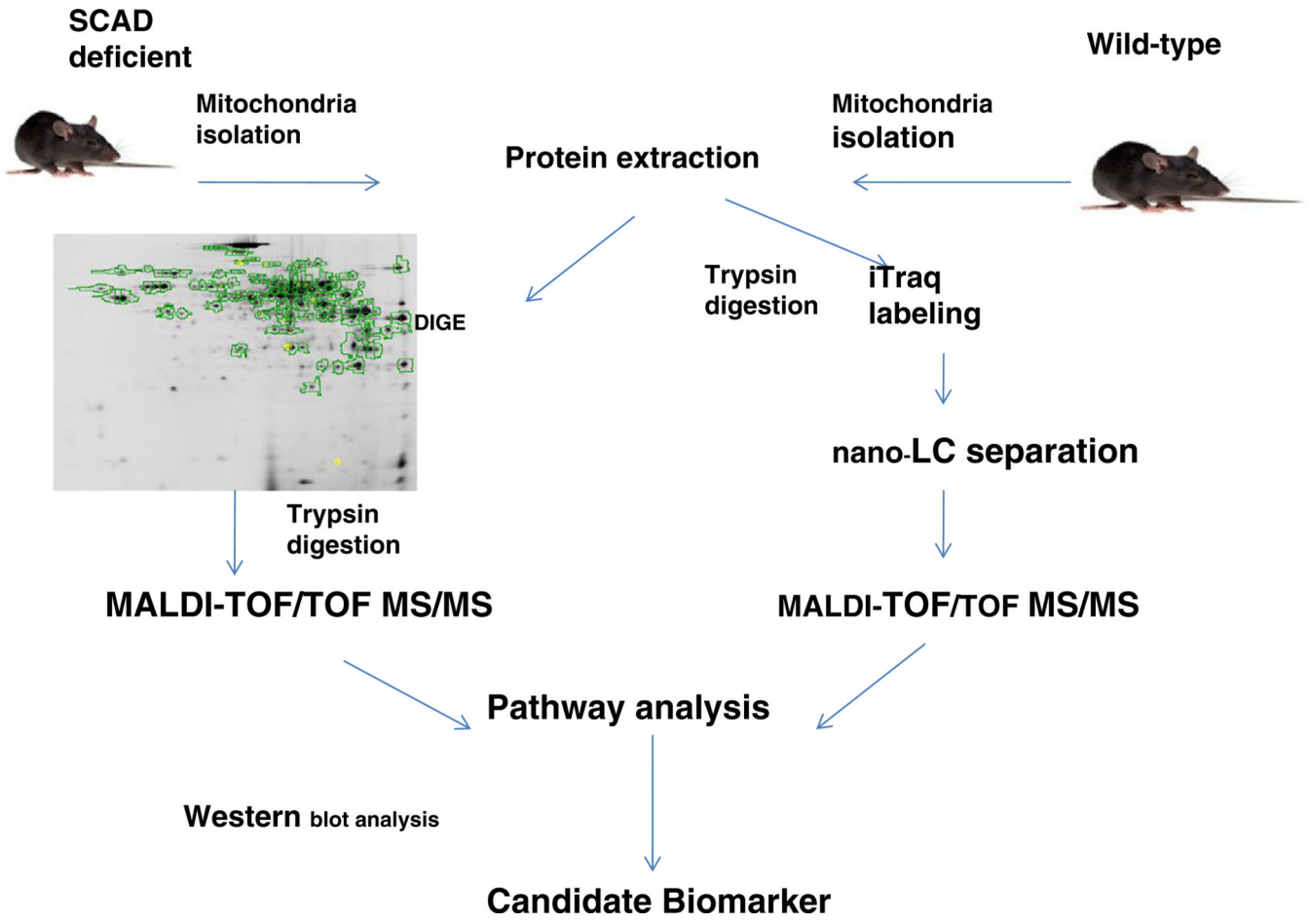

Fig. 1.
Schematic for proteomic experiments. See text for detailed description.

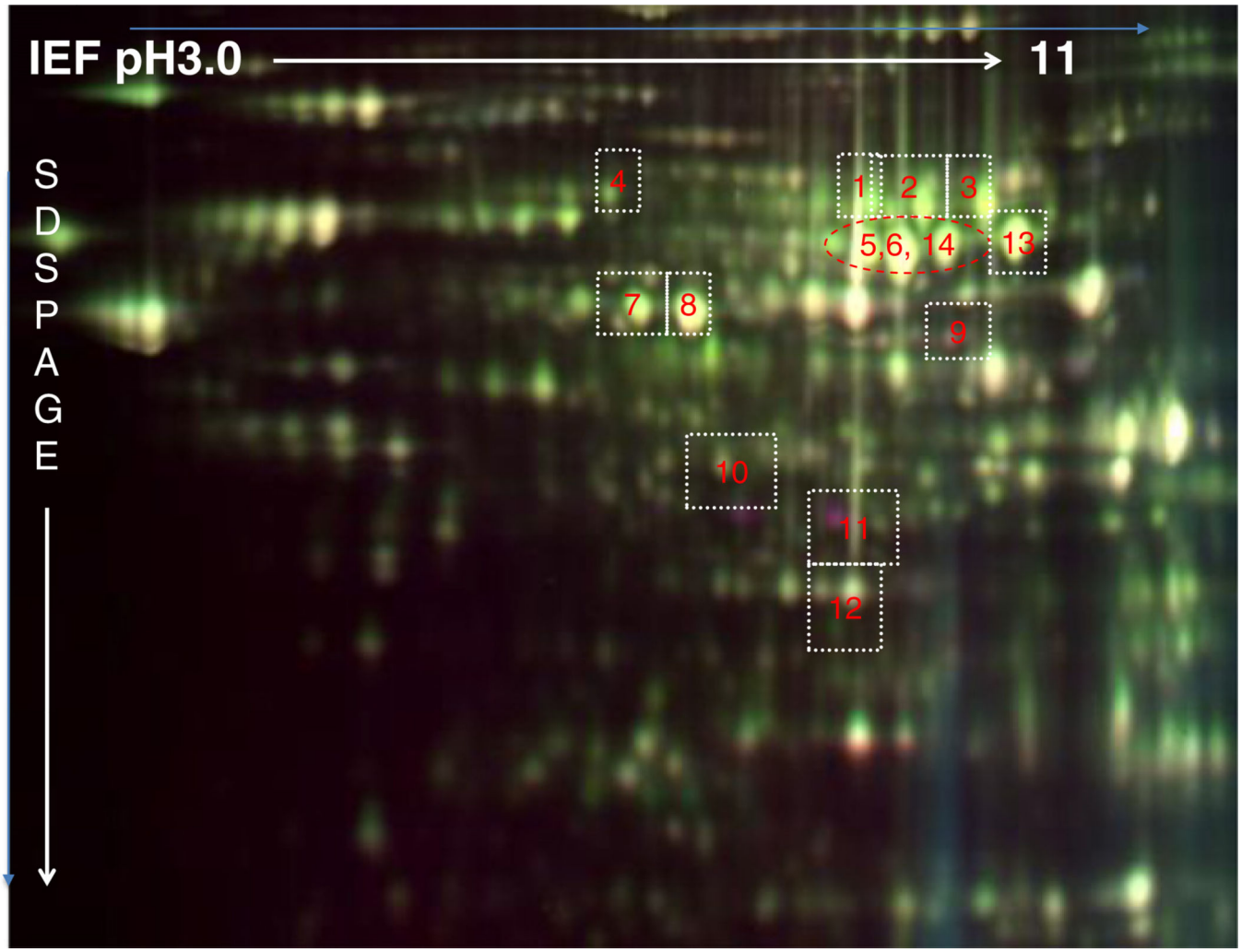

Fig. 2.

Representative 2DIGE image showing the significantly changed proteins in SCAD deficient mice. Mitochondrial proteins were separated in the first dimension by IEF with pH range from 3 to 11 then 12.5% SDS-polyacrylamide in the second dimension. Proteins from deficient and wild type mice were labeled with Cy3 or Cy5 in a reciprocal manner. In each gel, an internal standard from pooled samples was labeled with Cy2 to allow matching of spots in different gels and to normalize the amount of loaded protein. Protein spots that were differentially expressed (over 1.3 fold change, $p < 0.05$) and successfully identified with MALDI-TOF/TOF are marked with numbers.

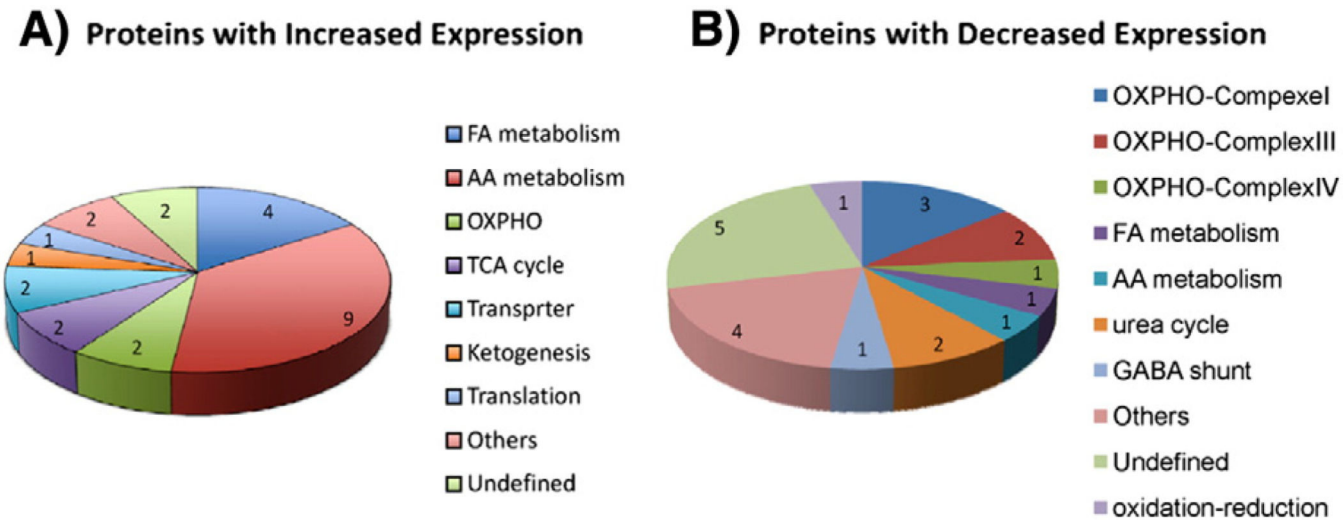

Fig. 3.

Functional distributions of differentially expressed proteins; (A) proteins increased in level; (B) proteins decreased in level. The number of proteins in each group of related biological functions is marked. Biological functions are as follows: fatty acid oxidation metabolism (FAO), amino acid metabolism (AA), lipid transfer or lipid metabolism (LM), protein folding or import (PFI), oxidative phosphorylation (OXPHOS), gene translation (GT), not any of the above (others) and undefined.

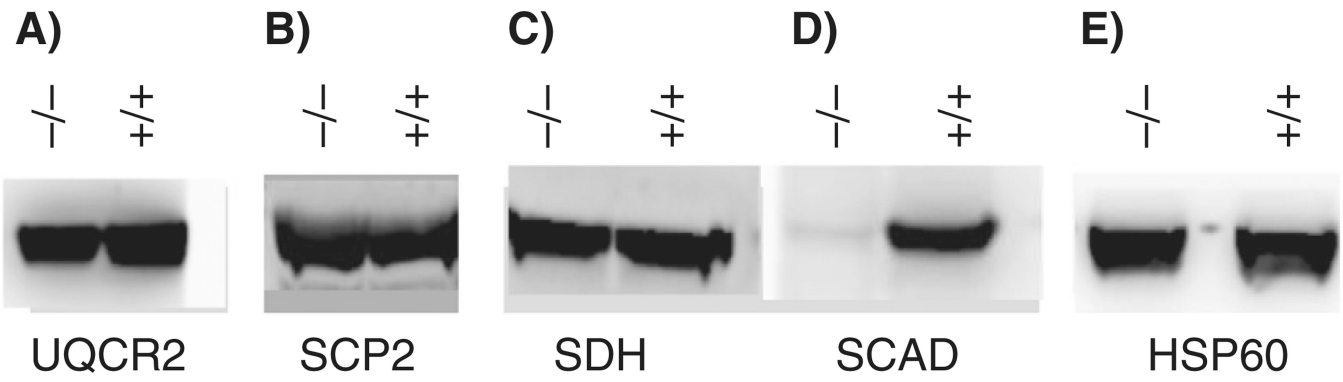

Fig. 4.

Western blot analyses of SCADD mouse liver extracts. A. cytochrome b–c1 complex subunit 2 using anti-UQCR2 antibody; B, sterol carrier protein 2 using anti-SCP2 antibody; C, succinate dehydrogenase (complex II) using anti-SDH antibody; D, SCAD using anti-SCAD antibody, and E, anti-heat shock protein 60 (HSP60) antiserum. Mitochondria proteins were isolated from SCAD deficient (−/−) and wild type (+/+) mouse livers. Samples were run on 10% polyacrylamide, Tris–Bis gels.

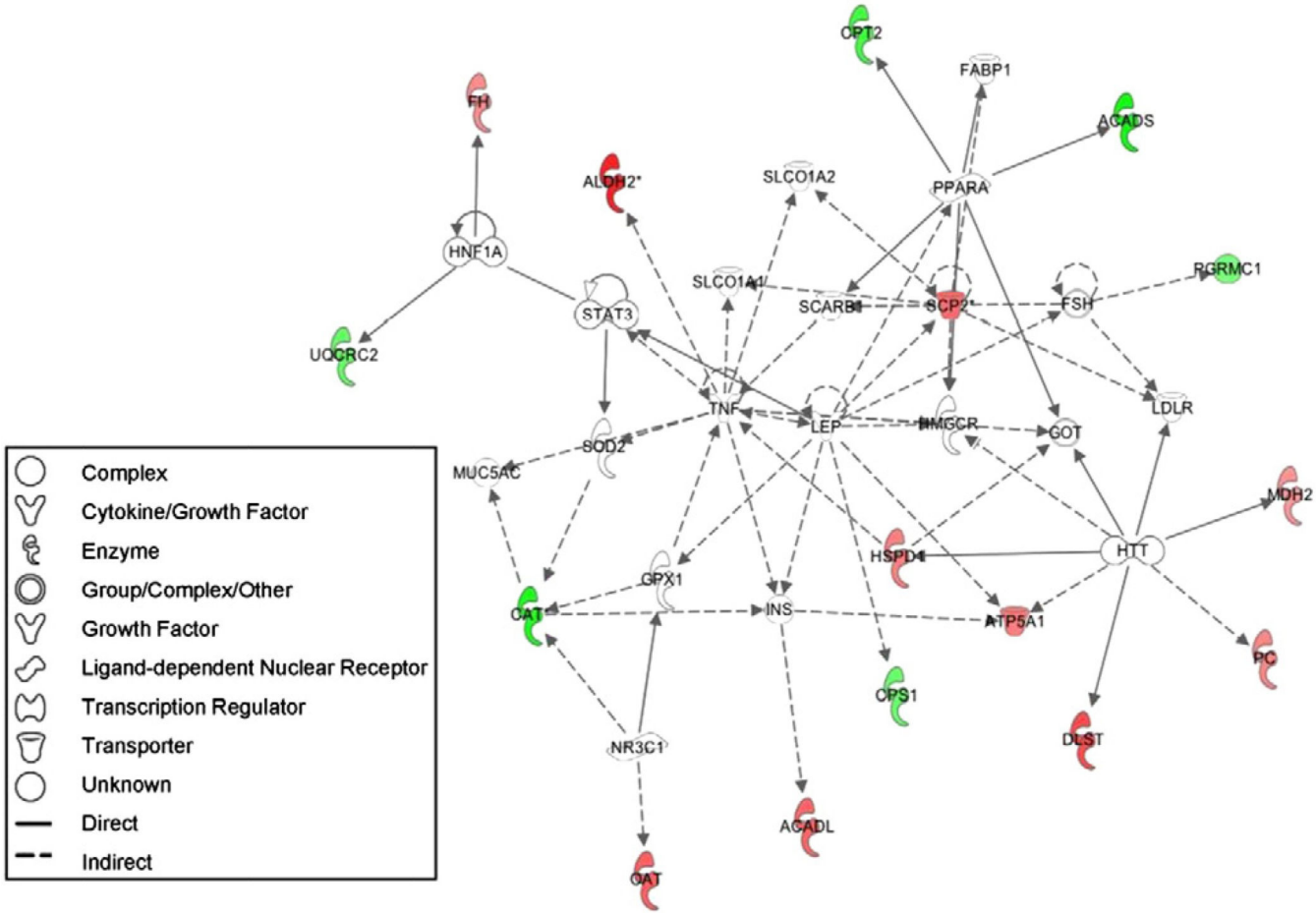

Fig. 5.

Top-rated network of lipid metabolism, molecular transport in SCADD mice. The network of “lipid metabolism, molecular transport” associated with altered proteins in SCAD deficient mice was generated and scored as the top-rated network by IPA. Red nodes indicate that the protein is up regulated in SCAD deficient mice. Proteins colored green indicate that the protein is down-regulated. The color intensity corresponds to the degree of abundance. Proteins in white are those identified through the Ingenuity Pathways Knowledge Base. The shapes denote the molecular class of the protein. A solid line indicates a direct molecular interaction, and a dashed line indicates an indirect molecular interaction. Gene designations are as follows: FH: fumarate hydratase; HNF1A: hepatocyte nuclear factor 1A; UQCRC2: unbiquinol-cytochrome c reductase core protein 2; TAT3 signal transducer and activator of transcription 3; MUC5AC: mucin 5, subtypes A and C; CAT: catalase; ALDH2: aldehyde dehydrogenase 2; SOD2: superoxide dismutase 2; GPX1: glutathione peroxidase; NR3C1: glucocorticoid receptor; OAT: ornithine amino transferase; SLCO1A2: solute carrier organic anion transporter family, member 1A2; TNF: tumor necrosis factor; INS: insulin ACADL: long chain acyl-CoA dehydro-genase; SCARB: spinocerebellar ataxia, autosomal recessive 2; LEP: leptin; CPS1: carbamoylphosphate synthetase 1; HSPD: Heat shock protein D; CPT2: carnitine palmitoyl transferase 2; PPARA: peroxisome proliferator-activate receptor-alpha; SCP2: sterol carrier protein 2;

HMGCR: 3-hydroxy-3-methylglutaryl-CoA reductase; ATP5A1: ATP synthase, H^+ transporting, mitochondrial F1 complex, alpha subunit; ACADS: short chain acyl-CoA dehydrogenase; FSH: follicle stimulating hormone; GOT: glutamate oxaloacetate transaminase, mitochondrial; HTT: huntingtin; DLST: dihydrolipoamide S-succinyltransferase; PGRMC1: progesterone receptor membrane component1;LDLR: low density lipoprotein receptor; MDH2: malate dehydrogenase, mitochondrial; PC: pyruvate carboxylase.

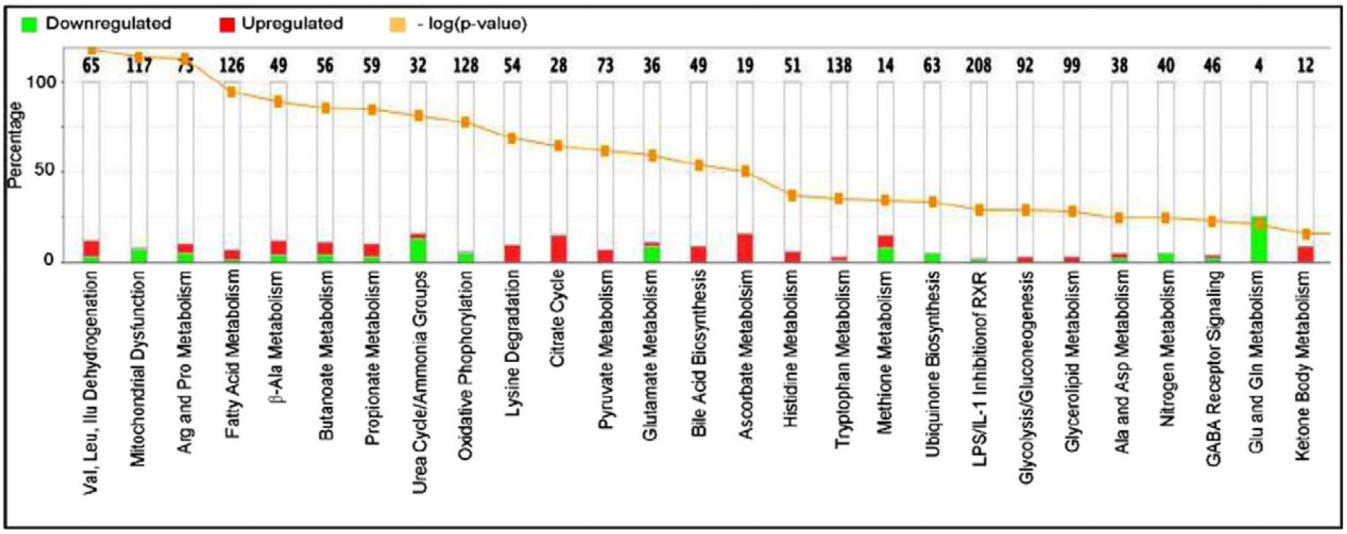

Fig. 6.

Pathways that are associated with changed proteins. Proteins are displayed along the x-axis. The y-axis displays the percentage which is calculated as follows: number of genes in a given pathway that meet cutoff criteria, divided by total number of genes that make up that pathway. The orange dotted line displays the significance of -log(p-value). Red denotes the gene/protein that is up-regulated, green denotes the gene/protein that is down-regulated.

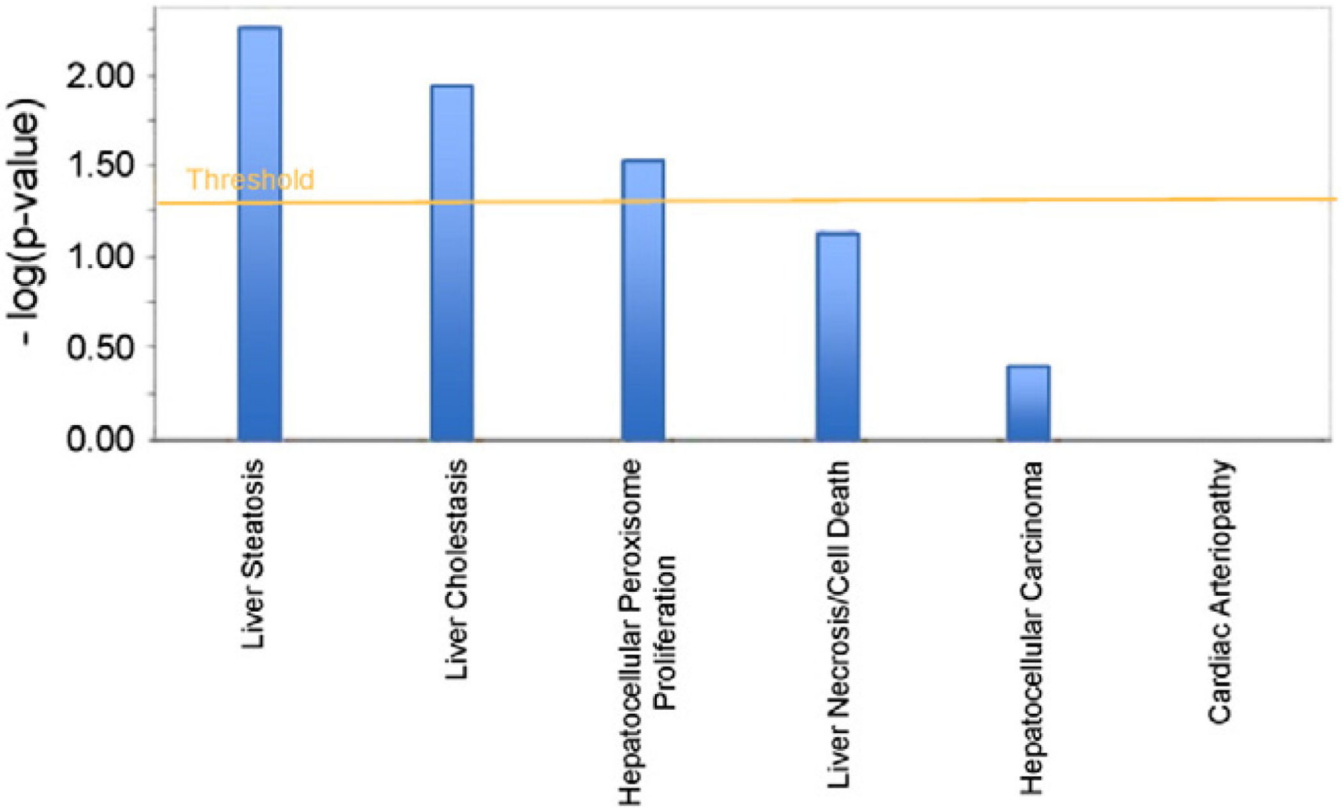

Fig. 7.

Hepatotoxicity of altered proteins indicating the clinical relevance of altered proteins. The figure displays a bar chart with the ingenuity toxicity on the x-axis and the significance [-log(p-value)] on the y-axis.

Table 1

Top 5 significantly associated diseases and disorders groups with altered proteins.

Diseases and disorders	p-Value	# of molecules
Neurologic disease	3.05 E-6–4.28 E-2	6
Metabolic disease	1.87 E-4–2.43 E-2	18
Endocrine system disorders	2.73 E-3–2.43 E-2	2
Genetic disorders	2.73 E-3–4.02 E-3	26
Hematologic disease	2.73 E-3–2.73 E-3	1

Table 2

Biomarkers identified in differentially expressed proteins.

Gene symbol	Entrez gene name	Family	GenPept/IPI/UniProt/Swiss-Prot accession	Fold change
ACAA2	Acetyl-CoA acyltransferase 2	Enzyme	IPI00653158.1	2.600
ACADL	Acyl-CoA dehydrogenase, long chain	Enzyme	IPI00894588.1	2.000
ACADS	Acyl-CoA dehydrogenase, C-2 to C-3 short chain	Enzyme	Q91W85	−3.580
ALDH2	Aldehyde dehydrogenase 2 family (mitochondrial)	Enzyme	IPI00111218.1	3.110
CPT2	Carnitine palmitoyltransferase 2	Enzyme	IPI00881401.1	−2.703
EPHX1	Epoxide hydrolase 1, microsomal (xenobiotic)	Peptidase	Q9D379	1.500
GLUD1	Glutamate dehydrogenase 1	Enzyme	IPI00114209.1	−2.041
PC	Pyruvate carboxylase	Enzyme	IPI00943457.1	1.560